

# Lepton flavor violating signals of the LHT model via $e^+e^-$ and $\gamma\gamma$ collisions at the ILC

Wei Ma, Chong-Xing Yue, Jiao Zhang, and Yan-Bin Sun

Department of Physics, Liaoning Normal University, Dalian, 116029 People's Republic of China \*

August 10, 2018

## Abstract

Taking into account the constraints on the free parameters of the littlest Higgs model with  $T$  parity (called the LHT model) from some rare decay processes, such as  $\mu \rightarrow e\gamma$  and  $\mu \rightarrow 3e$ , we consider the contributions of the LHT model to the lepton flavor violating (LFV) processes  $e^+e^- \rightarrow l_i\bar{l}_j$  and  $\gamma\gamma \rightarrow l_i\bar{l}_j$  ( $i \neq j$ ). We find that the LHT model can indeed produce significant contributions to these LFV processes and its LFV signal might have a chance of being observed in the future International Linear Collider experiments.

PACS number: 12.60.Cn, 11.30.Fs, 13.66.De

---

\*cxyue@lnnu.edu.cn

# I. Introduction

During the past decade, neutrino oscillation experiments have provided us with very convincing evidence that neutrinos are massive particles mixing with each other [1]. Moreover, their masses are extremely small, while mixing is nearly maximal, which means that the lepton flavor violating (LFV) processes are allowed. However, it is well known that, in the standard model (SM), neutrinos are massless and the LFV processes are not allowed at tree level. Thus, the exciting experimental fact opens a window to new physics beyond the SM [2]. In fact, lepton flavor symmetry is an accidental symmetry at low energy, and it may be violated beyond the SM. Many kinds of popular specific models, like supersymmetry, technicolor, and little Higgs models, indicate the possibility of large LFV. Therefore, an LFV signal in the charged lepton sector would be a clear hint for new physics beyond the SM. Experimental detection of the LFV phenomenon can provide an evidence of new physics.

Searching for new physics beyond the SM is one of the most important issues of current particle physics. The CERN Large Hadron Collider (LHC) can generate very massive new particles and will essentially enlarge the possibilities of testing for new physics effects. However, the LHC is a hadronic machine and precision measurements will be quite hard to undertake there. Also, the existence of large backgrounds at the LHC may hinder discoveries of new physical phenomena already possible at the energies that this accelerator will achieve. Thus, the next generation  $e^+e^-$  International Linear Collider (ILC) with the center of mass (c.m.) energy  $\sqrt{s} = 0.5 - 1 TeV$  and the typical integrated luminosity  $\mathcal{L}_{int} = 0.5 - 1 ab^{-1}$  is currently being designed [3, 4]. Because of its rather clean environment and high luminosity, the ILC will allow unambiguous precision measurements. In such a collider, in addition to  $e^+e^-$  collision, one can also realize  $\gamma\gamma$  collision with the photon beams generated by the backward Compton scattering of incident electron- and laser- beams. The  $\gamma\gamma$  collision offers a unique opportunity to explore new physics effects through production mechanisms which are not accessible in leptonic or hadronic machines [5].

It is well known that many popular models beyond the SM predict the presence of new particles, such as new gauge bosons, new fermions, and new scalars, which can generally enhance the branching ratios for some LFV decay processes, for instance  $l_i \rightarrow l_j \gamma$ ,  $l_i \rightarrow l_j l_k \bar{l}_l$ , and  $Z \rightarrow l_i \bar{l}_j$ . The upper experimental limits for some of these LFV decay processes can give serve constraints on the corresponding new physics models. Nevertheless, it is possible that the LFV signals may be observed at the ILC. This fact has lead to lot of work to study the LFV processes  $e^+ e^- \rightarrow l_i \bar{l}_j$  and  $\gamma \gamma \rightarrow l_i \bar{l}_j$  in the framework of specific models beyond the SM [6, 7] and in a model-independent manner [8]. Taking into account the constraints of the upper experimental limits for some LFV decay processes on the littlest Higgs model with  $T$  parity (called the LHT model) [9], in this paper, we will focus our attention on its contributions to the LFV processes  $e^+ e^- \rightarrow l_i \bar{l}_j$  and  $\gamma \gamma \rightarrow l_i \bar{l}_j$  ( $i \neq j$ ). We calculate the production cross sections of these processes induced by the LHT model and discuss the possibility of detecting the LFV signals of the LHT model via  $e^+ e^-$  and  $\gamma \gamma$  collisions at the ILC.

The rest of this paper is organized as follows. In Sec. II, we briefly review the essential features of the LHT model, which are related our calculation. A simple discussion about the constraints on the LHT model from some LFV decay processes is also given in this section. The production cross sections of the LFV processes  $e^+ e^- \rightarrow l_i \bar{l}_j$  and  $\gamma \gamma \rightarrow l_i \bar{l}_j$  are calculated in Secs. III and IV, respectively. Finally, the conclusions are given in Sec. V.

## II. The essential features of the LHT model

Little Higgs theory [10] was proposed as an alternative solution to the hierarchy problem of the SM, which provides a possible kind of electroweak symmetry breaking (EWSB) mechanism accomplished by a naturally light Higgs boson. In order to make the littlest Higgs model consistent with electroweak precision tests and simultaneously having the new particles of this model in the reach of the LHC, a discrete symmetry, T-parity, has been introduced, which forms the LHT model. The detailed description of the LHT model

can be found for instance in Refs.[9,11,12], and here we just want to briefly review its essential features, which are related to our calculation.

The LHT model is based on an  $SU(5)/SO(5)$  global symmetry breaking pattern. A subgroup  $[SU(2) \times U(1)]_1 \times [SU(2) \times U(1)]_2$  of the  $SU(5)$  global symmetry is gauged, and at the scale  $f$  it is broken into the SM electroweak symmetry  $SU(2)_L \times U(1)_Y$ . T-parity exchanges the  $[SU(2) \times U(1)]_1$  and  $[SU(2) \times U(1)]_2$  gauge symmetries. The T-even combinations of the gauge fields are the SM electroweak gauge bosons  $W_\mu^a$  and  $A_\mu$ . The T-odd combinations are T-parity partners of the SM electroweak gauge bosons.

After taking into account EWSB, at the order of  $v^2/f^2$ , the masses of the T-odd set of the  $SU(2) \times U(1)$  gauge bosons are given as

$$M_{B_H} = \frac{g_1 f}{\sqrt{5}} \left[ 1 - \frac{5v^2}{f^2} \right], \quad M_{Z_H} \approx M_{W_H} = g_2 f \left[ 1 - \frac{v^2}{8f^2} \right], \quad (1)$$

where  $v = 246 GeV$  is the electroweak scale and  $f$  is the scale parameter of the gauge symmetry breaking of the LHT model,  $g_1$  and  $g_2$  are the SM  $U(1)_Y$  and  $SU(2)_L$  gauge coupling constants, respectively.

A consistent implementation of T-parity also requires the introduction of mirror fermions — one for each quark and lepton species. The masses of the T-odd (mirror) fermions can be written in a unified manner:

$$M_{F_i} = \sqrt{2} k_i f, \quad (2)$$

where  $k_i$  are the eigenvalues of the mass matrix  $k$  and their values are generally dependent on the fermion species  $i$ . These new fermions (T-odd quarks and T-odd leptons) have new flavor violating interactions with the SM fermions mediated by the new gauge bosons ( $B_H, W_H^\pm$  and  $Z_H$ ) and at higher order by the triplet scalar  $\Phi$ . These interactions are governed by new mixing matrices  $V_{Hd}$  and  $V_{Hl}$  for down-type quarks and charged leptons, respectively. The corresponding matrices in the up-type quarks ( $V_{Hu}$ ) and neutrino ( $V_{H\nu}$ ) sectors are obtained by means of the relations:

$$V_{Hu}^+ V_{Hd} = V_{CKM}, \quad V_{H\nu}^+ V_{Hl} = V_{PMNS}. \quad (3)$$

Where the Cabibbo-Kobayashi-Maskawa (CKM) matrix  $V_{CKM}$  is defined through flavor mixing in the down-type quark sector, while the PMNS matrix  $V_{PMNS}$  is defined through neutrino mixing.

The Feynman rules of the LHT model have been studied in Ref.[12] and the corrected Feynman rules of Ref.[12] are given in Refs.[13, 14]. To simplify our paper, we do not list them here.

From the above discussions, we can see that the flavor structure of the LHT model is much richer than the one of the SM, mainly due to the presence of three doublets of mirror quarks and leptons and their interactions with the ordinary quarks and leptons. Such new flavor changing interactions can induce that the LHT model generates contributions to some flavor changing processes. The contributions of the LHT model to the LFV decay processes have been extensively studied and compared with current experimental limits in the literature [14,15,16]. It has been shown that the LHT model can enhance the SM prediction values by several orders of magnitude and the experimental measurement data for some LFV decay processes can give serve constraints on the free parameters of the LHT model.

The new particles predicted by the LHT model can generate significant contributions to the LFV decay process  $\mu \rightarrow 3e$  via box diagrams and the effective vertices  $\gamma(Z)e\bar{e}$  generated by  $\gamma$ - and  $Z$ -penguins, while only via  $\gamma$ - penguin for the LFV decay process  $\mu \rightarrow e\gamma$  [14, 15]. In order to suppress the values of the branching ratios  $Br(\mu \rightarrow e\gamma)$  and  $Br(\mu \rightarrow 3e)$  predicted by the LHT model below the present experimental upper bounds, the relevant mixing matrix  $V_{HI}$  must be rather hierarchical or mass splitting for the first and second  $T$ -odd lepton masses is very small. Reference [15] has shown that, for  $f = 1TeV$ , the mass splitting  $\Delta M = |M_{l_H^1} - M_{l_H^2}|$  must satisfy  $\Delta M \leq 40GeV$  and  $60GeV$  for assuming  $V_{HI} = V_{PMNS}$  and  $V_{HI} = V_{CKM}$ , respectively, in which  $M_{l_H^i}$  is the mass of the  $i$ -th generation  $T$ -odd lepton. It should be noted that the value of  $\Delta M$  increases as the scale parameter  $f$  increases. However, the present experimental upper bounds for  $\mu \rightarrow 3e$  and  $\mu \rightarrow e\gamma$  can not give significant constraints on the mass of the third  $T$ -odd lepton generation. Thus, in this paper, we will assume  $M_{l_H^1} = M_{l_H^2} = M_2$

and  $M_{l_H^3} = M_3$ . In our following numerical estimation, we take the mass parameters  $M_2$  and  $M_3$ , and the scale parameter  $f$  as free parameters.

### III. The LFV processes $e^+e^- \rightarrow l_i\bar{l}_j$ in the LHT model

From above discussions we can see that the LHT model can contribute to the LFV processes  $e^+e^- \rightarrow l_i\bar{l}_j$  ( $i \neq j$ ) via the effective vertices  $\gamma(Z)l_i\bar{l}_j$  and the box diagrams. The Feynman diagrams for the LFV processes  $e^+e^- \rightarrow l_i\bar{l}_j$  are depicted in Fig.1, in which  $\omega^{\pm,0}$  and  $\eta$  represent the would be Goldstone bosons arising from the LHT model. It is obvious that the contributions of the LHT model to this process mainly come from the effective vertices  $\gamma(Z)l_i\bar{l}_j$  [Fig.1(a)–Fig.1(k)], which are related the LFV processes  $\mu \rightarrow 3e$  and  $\mu \rightarrow e\gamma$ . Thus, the production cross sections of the processes  $e^+e^- \rightarrow l_i\bar{l}_j$  should also be constrained by the present experimental upper bounds of these processes. However, as shown in Refs.[14, 15], as long as  $\Delta M \approx 0$ , the LHT model can satisfy the constrains from  $\mu \rightarrow 3e$  and  $\mu \rightarrow e\gamma$ . The constraints on other free parameters, such as the mass  $M_3$  of the third  $T$ -odd lepton generation, the mixing matrix elements  $(V_{Hl})_{ij}$ , etc. are very weak. So, it is possible that the LHT model can give sizable cross sections for the processes  $e^+e^- \rightarrow l_i\bar{l}_j$ . Our calculation has shown that it is indeed this case.

The one-loop calculation can be carried out by summing all of these one-loop diagrams and the results will be finite and gauge invariant. Each loop diagram is composed of some scalar loop functions, which are calculated by using *LoopTools* [17]. In the following sections, we will use the 't Hooft-Feynman gauge to calculate their production cross sections. Because the calculation of the loop diagrams is too tedious and the analytical expressions are lengthy, we will not present them here.

It is obvious that, except for the SM input parameters  $\alpha = 1/128.8$ ,  $S_W^2 = 0.2315$ , and  $M_Z = 91.187\text{GeV}$  [18], the production cross sections  $\sigma_{ij}$  for the LFV processes  $e^+e^- \rightarrow l_i\bar{l}_j$  are dependent on the model dependent parameters  $(V_{Hl})_{ij}$ ,  $f$ , and the  $T$ -odd leptons' masses. The matrix elements  $(V_{Hl})_{ij}$  can be determined through  $V_{Hl} = V_{H\nu}V_{PMNS}$ . To avoid any additional parameters introduced and to simplify our calculations, we take

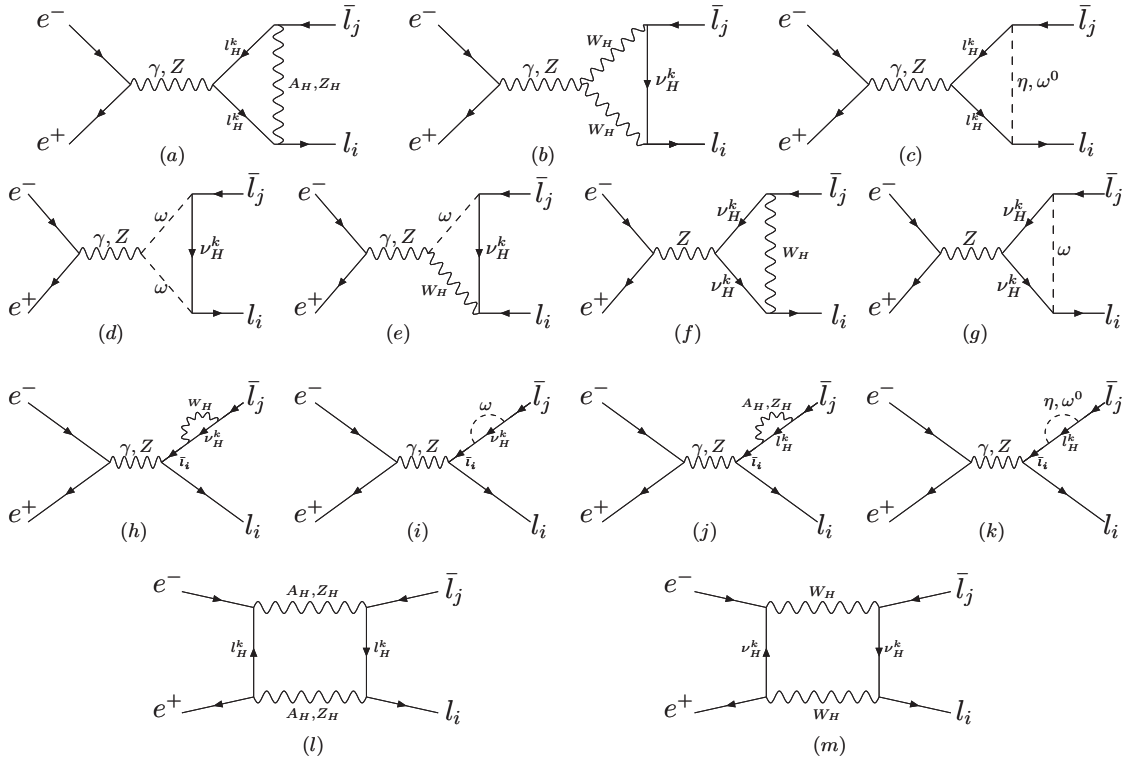


Figure 1: The Feynman diagrams for the LFV processes  $e^+e^- \rightarrow l_i \bar{l}_j$  in the LHT model.

$V_{Hl} = V_{PMNS}$ , which means that  $V_{H\nu} = I$  and the  $T$ -odd leptons have no effects on the flavor violating observable in the neutrino sector [14, 19]. Certainly, this is a very limited scenario. However, in order to satisfy the constraints from  $\mu \rightarrow 3e$  and  $\mu \rightarrow e\gamma$ , the mixing matrix  $V_{Hl}$  must be rather hierarchical or the first and second  $T$ -odd lepton masses are quasidegenerate. Therefore, in this paper, we take  $M_{l_H^1} = M_{l_H^2}$  and  $V_{Hl} = V_{PMNS}$  might be suitable. For the PMNS matrix  $V_{PMNS}$ , we take the standard parametrization form with parameters given by the neutrino experiments [20]. Since there is not constraints on the PMNS phases, we will take the Dirac phase to be equal to the CKM phase and set the two Majorana phases to zero in our numerical estimations.

Our numerical results are summarized in Fig.2, in which we plot the production cross sections  $\sigma_{ij}$  as functions of the mass parameter  $M_3$  for  $M_2 = 400\text{GeV}$  and three values of the scale parameter  $f$ . Figures(a), Fig.2(b) and Fig.2(c) are corresponding to the

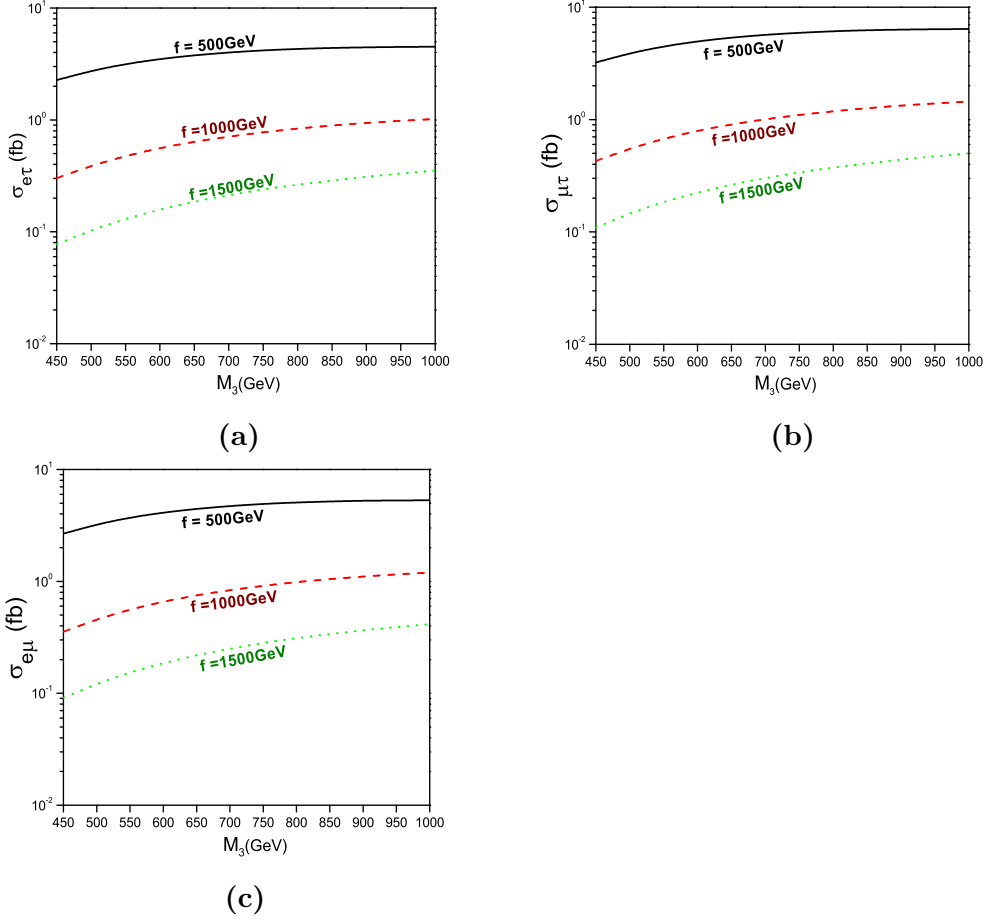


Figure 2: The production cross sections  $\sigma_{ij}$  for the processes  $e^+e^- \rightarrow l_i\bar{l}_j$  as function of the mass parameter  $M_3$  for  $M_2 = 400\text{GeV}$  and three values of the scale parameter  $f$

LFV processes  $e^+e^- \rightarrow e\bar{\tau}$ ,  $e^+e^- \rightarrow \mu\bar{\tau}$  and  $e^+e^- \rightarrow e\bar{\mu}$ , respectively. In these figures, we have taken the c. m. energy  $\sqrt{s} = 500\text{GeV}$ . One can see from Fig.2 that the contributions of the LHT model to the LFV processes  $e^+e^- \rightarrow l_i\bar{l}_j$  ( $i \neq j$ ) increase as the third family  $T$ -odd lepton mass  $M_3$  increases and the scale parameter  $f$  decreases. In most of the parameter space, the production cross sections for the states  $e\bar{\tau}$ ,  $\mu\bar{\tau}$  and  $e\bar{\mu}$  are approximately at the same order of magnitude. For  $\sqrt{s} = 500\text{GeV}$ ,  $M_2 = 400\text{GeV}$ ,  $450\text{GeV} \leq M_3 \leq 1000\text{GeV}$  and  $500\text{GeV} \leq f \leq 1500\text{GeV}$ , there are  $0.08\text{fb} \leq \sigma_{e\bar{\tau}} \leq 4.5\text{fb}$ ,  $0.1\text{fb} \leq \sigma_{\mu\bar{\tau}} \leq 6.4\text{fb}$  and  $0.09\text{fb} \leq \sigma_{e\bar{\mu}} \leq 5.3\text{fb}$ , respectively. If we assume the integrated luminosity  $\mathcal{L}_{int} = 500\text{fb}^{-1}$ , there will be several tens and up to thousands of  $l_i\bar{l}_j$  events



to be generated in the future ILC experiments.

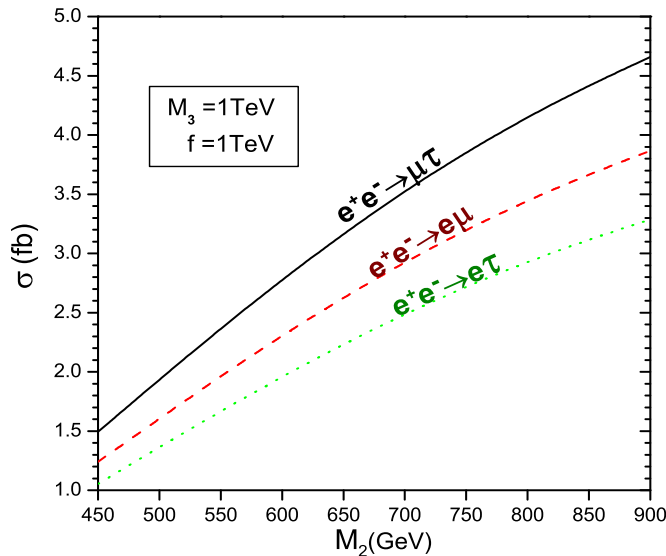


Figure 3: The production cross sections  $\sigma_{ij}$  for the processes  $e^+e^- \rightarrow l_i\bar{l}_j$  as function of the mass parameter  $M_2$  for  $f = 1TeV$  and  $M_3 = 1000GeV$ .

To see the effect of the first and second generation  $T$ -odd lepton masses on the production cross sections  $\sigma_{ij}$ , in Fig.3, we plot  $\sigma_{ij}$  as functions of the mass parameter  $M_2$  for  $f = 1TeV$  and  $M_3 = 1000GeV$ . From Fig.3 one can see that the contributions of the LHT model to the LFV processes  $e^+e^- \rightarrow l_i\bar{l}_j$  also increase as the mass parameter  $M_2$ . For  $M_3 = 1000GeV$ ,  $f = 1TeV$ ,  $450GeV \leq M_2 \leq 900GeV$  and  $\sqrt{s} = 500GeV$ , they are  $1.1fb \leq \sigma_{e\bar{\tau}} \leq 3.3fb$ ,  $1.5fb \leq \sigma_{\mu\bar{\tau}} \leq 4.7fb$  and  $1.2fb \leq \sigma_{e\bar{\mu}} \leq 3.9fb$ , respectively.

It is well known that, at the ILC, the LFV production processes can provide extremely clear signatures and are experimentally interesting. For the three LFV processes  $e^+e^- \rightarrow e\bar{\tau}$ ,  $e^+e^- \rightarrow \mu\bar{\tau}$  and  $e^+e^- \rightarrow e\bar{\mu}$ , the final leptons always emerge back to back and carrying a constant energy which is one-half of the c.m. energy  $\sqrt{s}$ . The last process is the best one and almost free of the SM backgrounds. For the first and second production processes, we can assume the lepton tau decay  $\bar{\tau} \rightarrow \bar{\mu}\nu_\mu\bar{\nu}_\tau$  and  $\bar{\tau} \rightarrow \bar{e}\nu_e\bar{\nu}_\tau$ , which give rise to the signal events with opposite-sign and different-flavor leptons and missing energy ( $e\bar{\mu} + \cancel{E}$  and  $\mu\bar{e} + \cancel{E}$ ). Although this kind of LFV signal is quite spectacular, it is not free of the

SM backgrounds. For example, the leading backgrounds of the signal  $e\bar{\mu} + \cancel{E}$  mainly come from the SM processes  $e^+e^- \rightarrow e\bar{\mu}\nu_\mu\bar{\nu}_e$  and  $e^+e^- \rightarrow \tau^+\tau^- \rightarrow e\bar{\mu}\nu_\mu\bar{\nu}_e\nu_\tau\bar{\nu}_\tau$ , which have been discussed in Ref.[8]. They have shown that, with suitable cuts, the SM backgrounds can be largely suppressed. Thus, it is possible to observe the LFV signal of the LHT model in the future ILC experiments. Certainly, detailed study of the relevant backgrounds is needed, which is beyond the scope of this paper.

## IV. The LFV processes $\gamma\gamma \rightarrow l_i\bar{l}_j$ in the LHT model

It is well known that the ILC could offer the possibility of working in the  $\gamma\gamma$  or  $e\gamma$  collision thus realizing a very high energy photon collider [5]. For some production processes, their cross sections at the  $\gamma\gamma$  collider might be larger than the corresponding  $e^+e^-$  ones; this collider will reveal crucial information about these production processes. To see whether the LHT model can give significant contributions to the LFV final states  $l_i\bar{l}_j$  ( $i \neq j$ ) via  $\gamma\gamma$  collision, we will consider the LFV processes  $\gamma\gamma \rightarrow l_i\bar{l}_j$  in this section.

From the discussions given in Sec.II, we can see that the LHT model can only induce the LFV processes  $\gamma\gamma \rightarrow l_i\bar{l}_j$  at loop level. The relevant Feynman diagrams are shown in Fig.4. The Feynman diagrams created by exchanging the initial photons, which are not shown in Fig.4, are also involved in our calculations.

We use  $\theta$  to denote the scattering angle between one of the photons and one of the final leptons. Then, in the center of mass (c.m.) system, we express all the four-momenta of the initial and final particles by means of the  $\gamma\gamma$  c.m. energy  $\sqrt{\hat{s}}$  and the scattering angle  $\theta$ . The four-momentum components  $(E, p_x, p_y, p_z)$  of final particles  $l_i$  and  $\bar{l}_j$  can be written as

$$p_1 = (E_{l_i}, \sqrt{E_{l_i}^2 - m_{l_i}^2} \sin \theta, 0, \sqrt{E_{l_i}^2 - m_{l_i}^2} \cos \theta), \quad (4)$$

$$p_2 = (E_{\bar{l}_j}, -\sqrt{E_{\bar{l}_j}^2 - m_{\bar{l}_j}^2} \sin \theta, 0, -\sqrt{E_{\bar{l}_j}^2 - m_{\bar{l}_j}^2} \cos \theta), \quad (5)$$

where  $E_{l_i} = E_{\bar{l}_j} = \sqrt{\hat{s}}/2$ . The Mandelstam variables are defined as

$$\begin{aligned}\hat{s} &= (k_1 + k_2)^2 = (p_1 + p_2)^2, \\ \hat{t} &= (k_1 - p_1)^2 = (k_2 - p_2)^2, \\ \hat{u} &= (k_1 - p_2)^2 = (k_2 - p_1)^2.\end{aligned}$$

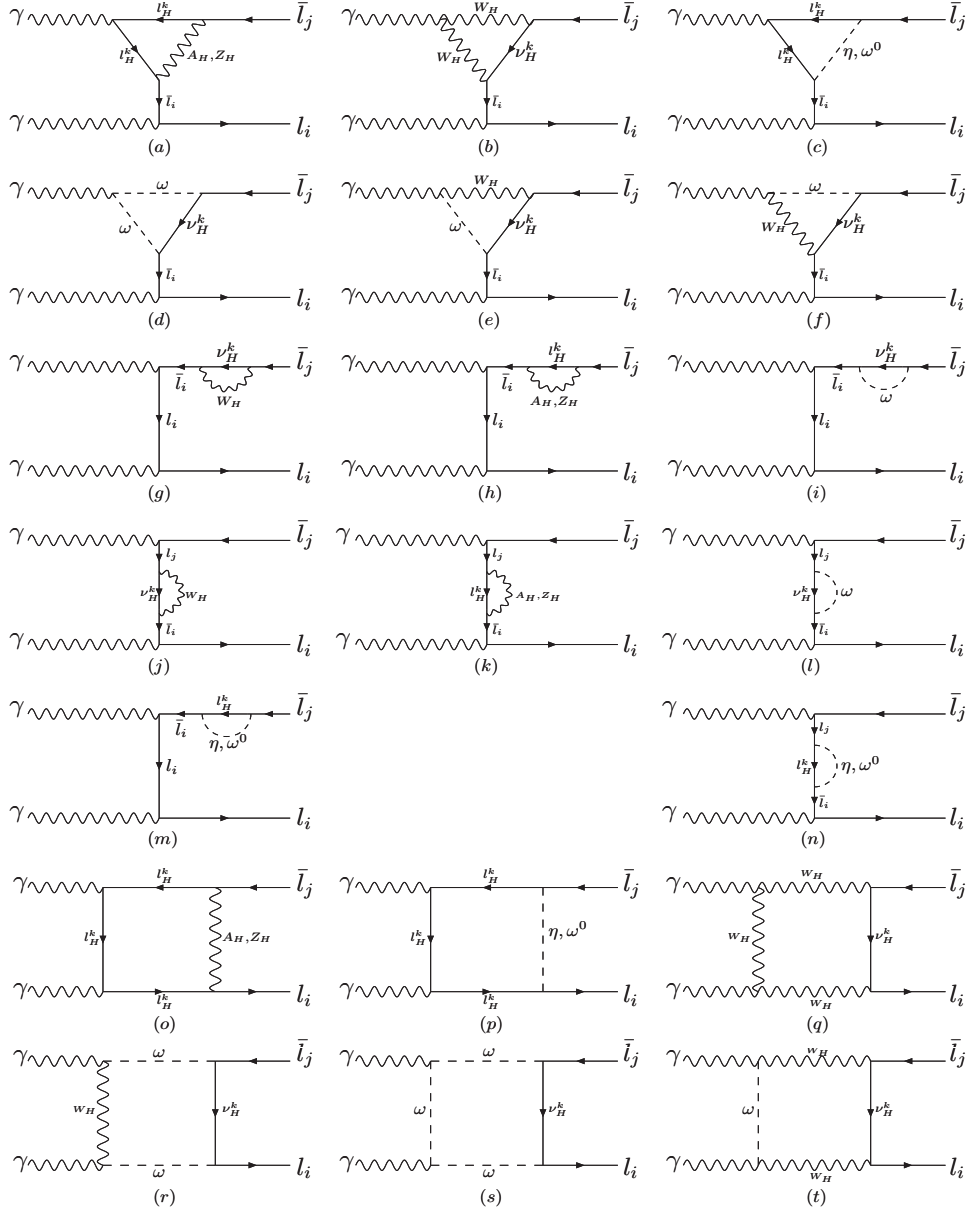


Figure 4: The Feynman diagrams for the LFV processes  $\gamma\gamma \rightarrow l_i\bar{l}_j$  in the LHT model.

The diagrams obtained by exchanging the initial photons are not shown here.

Where  $k_1$  and  $k_2$  are the 4-momenta of the initial photons, which can be written as

$k_1 = (\sqrt{\hat{s}}/2, 0, 0, \sqrt{\hat{s}}/2)$  and  $k_2 = (\sqrt{\hat{s}}/2, 0, 0, -\sqrt{\hat{s}}/2)$ . With the above definitions, we can give the renormalized amplitudes of the LFV processes  $\gamma\gamma \rightarrow l_i l_j$ . To simplify our paper, we do not give their explicit expressions here. The cross section for the LFV process  $\gamma\gamma \rightarrow l_i l_j$  can be generally expressed in the form

$$\hat{\sigma}(\hat{s}) = \frac{1}{16\pi\hat{s}^2} \int_{\hat{t}^-}^{\hat{t}^+} d\hat{t} \overline{\sum_{spin}} |\mathcal{M}|^2, \quad (6)$$

where  $\hat{t}^\pm = \frac{1}{2}[(m_{l_i}^2 + m_{l_j}^2 - \hat{s}) \pm \sqrt{(m_{l_i}^2 + m_{l_j}^2 - \hat{s})^2 - 4m_{l_i}^2 m_{l_j}^2}]$ , and the bar over summation means to take the average over the initial polarizations of the photons.

At the ILC, the effective cross section of the subprocess  $\gamma\gamma \rightarrow l_i \bar{l}_j$  can be written as

$$\sigma(s) = \int_{E_0/\sqrt{s}}^{x_{max}} dz \frac{d\mathcal{L}_{\gamma\gamma}}{dz} \hat{\sigma}_{\gamma\gamma \rightarrow l_i \bar{l}_j}(\hat{s} = z^2 s), \quad (7)$$

where  $E_0 = m_{l_i} + m_{\bar{l}_j}$ , and  $\sqrt{s}(\sqrt{\hat{s}})$  is the  $e^+e^- (\gamma\gamma)$  c.m. energy;  $d\mathcal{L}_{\gamma\gamma}/dz$  is the photon-beam luminosity distribution, which is defined as

$$\frac{d\mathcal{L}_{\gamma\gamma}}{dz} = 2z \int_{z^2/x_{max}}^{x_{max}} \frac{dx}{x} F_{\gamma/e}(x) F_{\gamma/e}(z^2/x). \quad (8)$$

For the initial unpolarized electron and laser-photon beams, the energy spectrum of the backscattered photon is given by [21]

$$F_{\gamma/e}(x) = \frac{1}{D(\xi)} \left[ 1 - x + \frac{1}{1-x} - \frac{4x}{\xi(1-x)} + \frac{4x^2}{\xi^2(1-x)^2} \right] \quad (9)$$

with

$$D(\xi) = \left( 1 - \frac{4}{\xi} - \frac{8}{\xi^2} \right) \ln(1 + \xi) + \frac{1}{2} + \frac{8}{\xi} - \frac{1}{2(1 + \xi)^2}, \quad (10)$$

where  $\xi = 4E_0\omega_0/m_e^2$ ,  $m_e$  and  $E_0$  are the incident electron mass and energy, respectively.  $\omega_0$  is the laser-photon energy,  $x$  is the fraction of the energy of the incident electron carried by the backscattered photon. In order to spoil the creation of  $e^+e^-$  pair by the interaction of the incident and backscattered photons, in our calculation, we require  $\omega_0 x_{max} \leq m_e^2/E_e$ , which implies  $\xi \leq 4.8$ . For the choice  $\xi = 4.8$ , there are  $x_{max} \simeq 0.83$  and  $D(\xi) = 1.8$ .

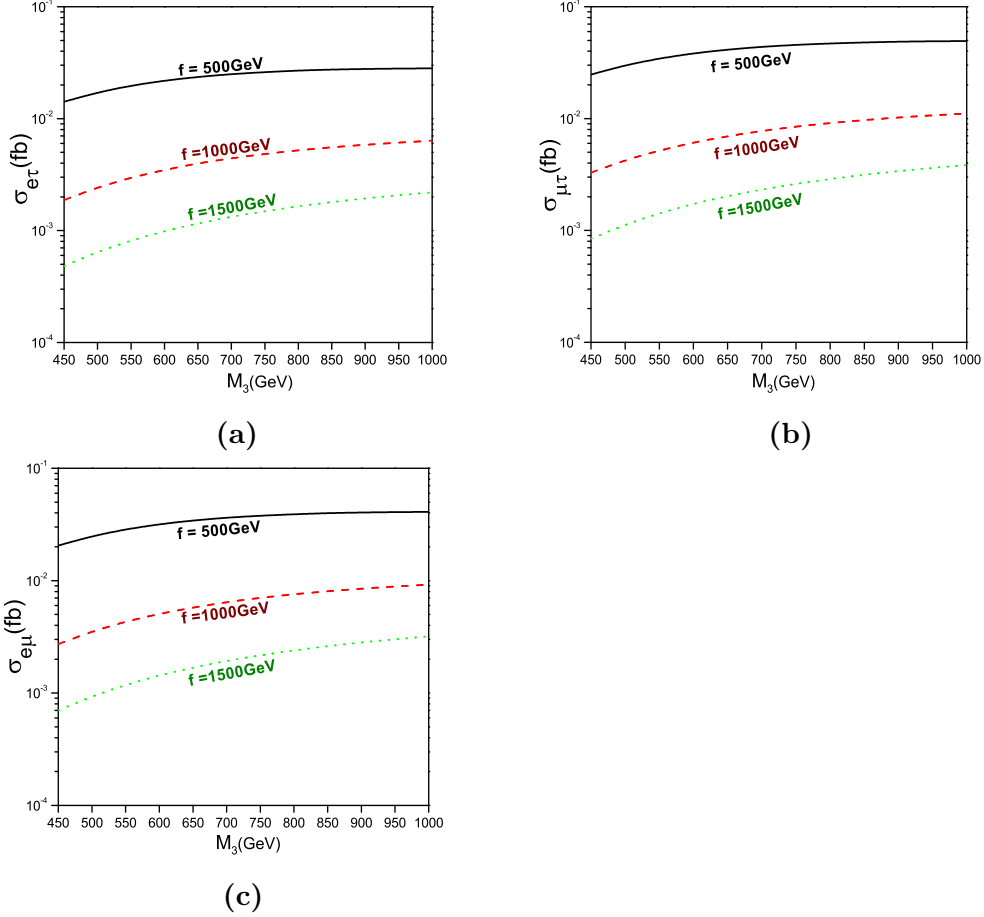


Figure 5: The production cross sections  $\sigma_{ij}$  for the subprocesses  $\gamma\gamma \rightarrow l_i \bar{l}_j$  as functions of the mass parameter  $M_3$  for  $M_2 = 400\text{GeV}$  and three values of the scale parameter  $f$ .

Similarly with Sec.III, we also assume  $V_{H\nu} = I$  and that the masses of the first generation  $T$ -odd fermions are equal to those of the second generation  $T$ -odd fermions. In this case, our numerical results are summarized in Figs.5 and Fig.6. Figure 5 plots the effective production cross sections  $\sigma_{ij}$  as functions of the mass parameter  $M_3$  for  $M_2 = 400\text{GeV}$  and three values of the scale parameter  $f$ , while Fig.6 plots the cross sections  $\sigma_{ij}$  as functions of  $M_2$  for  $f = 500\text{GeV}$  and  $M_3 = 1000\text{GeV}$ . One can see from these figures that, in most of the parameter space, the contributions of the LHT model to the LFV processes  $e^+e^- \rightarrow \gamma\gamma \rightarrow l_i \bar{l}_j$  are smaller than those for the LFV processes  $e^+e^- \rightarrow l_i \bar{l}_j$ . With the increasing of the mass parameter  $M_i$  and the decreasing of the scale

parameter  $f$ , the effective cross sections of the LFV processes  $\gamma\gamma \rightarrow l_i\bar{l}_j$  become larger. Such a behavior is similar to that for the LFV processes  $e^+e^- \rightarrow l_i\bar{l}_j$ . For  $\sqrt{s} = 500\text{GeV}$ ,  $M_2 = 400\text{GeV}$ ,  $450\text{GeV} \leq M_3 \leq 1000\text{GeV}$  and  $500\text{GeV} \leq f \leq 1500\text{GeV}$ , there are  $6 \times 10^{-4}\text{fb} \leq \sigma_{e\bar{\tau}} \leq 3 \times 10^{-2}\text{fb}$ ,  $8 \times 10^{-4}\text{fb} \leq \sigma_{\mu\bar{\tau}} \leq 5 \times 10^{-2}\text{fb}$  and  $7 \times 10^{-4}\text{fb} \leq \sigma_{e\bar{\mu}} \leq 4 \times 10^{-2}\text{fb}$ , respectively. There will be several tens of  $l_i\bar{l}_j$  events to be generated in the future ILC experiment with  $\mathcal{L}_{int} = 500\text{fb}^{-1}$  and  $\sqrt{s} = 500\text{GeV}$ .

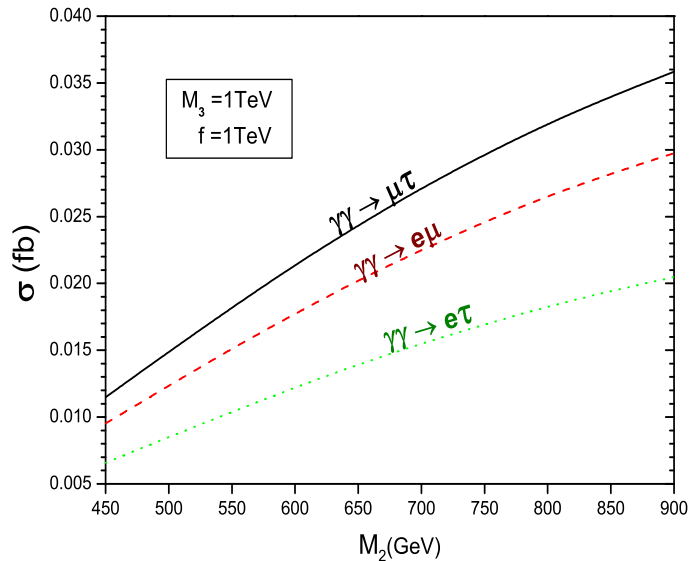


Figure 6: The production cross sections  $\sigma_{ij}$  for the subprocesses  $\gamma\gamma \rightarrow l_i\bar{l}_j$  as functions of the mass parameter  $M_2$  for  $f = 1\text{TeV}$  and  $M_3 = 1000\text{GeV}$ .

Similar with the LFV process  $e^+e^- \rightarrow e\bar{\mu}$ , the LFV process  $\gamma\gamma \rightarrow e\bar{\mu}$  is almost free of the SM background. For the LFV processes  $\gamma\gamma \rightarrow e\bar{\tau}$  and  $\gamma\gamma \rightarrow \mu\bar{\tau}$ , the SM backgrounds mainly come from the processes  $\gamma\gamma \rightarrow \tau^+\tau^-$  and  $\gamma\gamma \rightarrow WW$  with the lepton  $\tau$  and the electroweak gauge boson  $W$  leptonic decaying. It has been shown that, by applying appropriate kinematical cuts, the backgrounds can be significantly suppressed and the ratio of signal to background would be enhanced [6]. Thus, the LFV signatures of the LHT model might have a chance of being observed via the subprocesses  $\gamma\gamma \rightarrow l_i\bar{l}_j$  in the future ILC experiments.

## V. Conclusions and discussions

The LHT model is one of the attractive little Higgs models. To simultaneously implement  $T$ -parity, the LHT model introduces new mirror fermions ( $T$ -odd quarks and  $T$ -odd leptons). The flavor mixing in the mirror fermion sector gives rise to a new source of flavor violation, which might generate significant contributions to some flavor violation processes.

The evidence for the neutrino masses and flavor mixing, which can be seen as the first experimental clue of new physics beyond the SM, implies the nonconservation of the lepton flavor symmetry. Thus, the LFV processes related charged leptons are expected, which are very sensitive to new physics beyond the SM. Taking into account the constraints on the free parameters of the LHT model from the rare decay processes  $\mu \rightarrow e\gamma$  and  $\mu \rightarrow 3e$ , in this paper, we have considered the contributions of the LHT model to the LFV processes  $e^+e^- \rightarrow l_i\bar{l}_j$  and  $\gamma\gamma \rightarrow l_i\bar{l}_j$  ( $i \neq j$ ), which are induced at the one-loop level and will be of interest for the future ILC experiments. We find that, in wide range of the parameter space, the production cross section of the LFV process  $e^+e^- \rightarrow l_i\bar{l}_j$  can reach several  $fb$ , and that of the LFV process  $\gamma\gamma \rightarrow l_i\bar{l}_j$  can reach the order of magnitude of  $10^{-2}fb$ . This means that there will be several and up to thousands of  $l_i\bar{l}_j$  events to be generated each year for the designed luminosity of  $\mathcal{L}_{int} = 500fb^{-1}$  at the ILC. Since the production rate of these LFV processes predicted by the SM is almost negligible, the observation of such  $l_i\bar{l}_j$  events would be a robust evidence of the LHT model. Therefore, these LFV processes may serve as a sensitive probe of the LHT model.

An important tool of the ILC is the use of the polarized beams. One expects that a high polarization degree between 80% and 90% can be reached [3,4]. Beam polarization is not only useful for a possible reduction of the background, but might also serve as a possible tool to disentangle different contributions to the signal and to directly analyze the interaction structure of new physics models. In our calculation, we have not considered the polarization of the incident electron. Certainly, if we consider this case, our numerical results will be changed. Furthermore, we can also assume  $V_{Hl} = V_{CKM}$ , which makes the

values of the production cross sections of the LFV processes  $e^+e^- \rightarrow l_i\bar{l}_j$  different from those for assuming  $V_{Hl} = V_{PMNS}$ . However, our physical conclusions are not changed.

It is obvious that the production cross sections of the LFV processes  $e^+e^- \rightarrow l_i\bar{l}_j$  and  $\gamma\gamma \rightarrow l_i\bar{l}_j$  are dependent on the factor  $\Sigma_\alpha V_{Hl}^{\alpha i*} V_{Hl}^{\alpha j}$  with  $\alpha = 1, 2, 3$ . For assuming  $V_{Hl} = V_{PMNS}$ , the PMNS phases should have effects on these cross sections. In our numerical estimations, we have fixed the values of the PMNS phases. If we vary these values, the numerical results for the cross sections  $\sigma_{e\bar{\tau}}$ ,  $\sigma_{\mu\bar{\tau}}$  and  $\sigma_{e\bar{\mu}}$  are also changed. However, these variations are not significantly large. Our physical conclusions are not changed.

The  $T$ -odd quarks predicted by the LHT model also have new flavor violating interactions with the SM fermions mediated by the new gauge bosons and at higher order by the triplet scalar. These interactions are governed by the new mixing matrix  $V_{Hd}$  for down-quarks. So the  $T$ -odd quark sector can also generate significant contributions to some flavor changing processes [12, 13, 22, 23]. For example, Ref.[24] has shown that it is possible to test the signatures of the LHT model at the ILC and LHC experiments via the flavor changing processes  $e^+e^- \rightarrow \bar{t}c$ ,  $\gamma\gamma \rightarrow \bar{t}c$  and  $pp \rightarrow \bar{t}c$ .

The  $T$ -odd particles predicted by the LHT model can only be produced in pairs and give the direct signals at the LHC, which have close resemblance with those of supersymmetry with conserved  $R$  parity or universal extra dimensions with  $KK$  parity. The possibility of observing the  $T$ -odd leptons at the LHC has been studied in Ref.[25]. If the  $T$ -odd leptons are found at the LHC, we expect that our work will be helpful to determine their masses and couplings with high accuracy at the ILC.

## Acknowledgments

This work was supported in part by the National Natural Science Foundation of China under Grants No.10975067, the Specialized Research Fund for the Doctoral Program of Higher Education (SRFDP) (No.200801650002).



## References

- [1] C. K. Jung *et al.*, *Annu. Rev. Nucl. Part. Sci.* **51**, 451 (2001); Q. R. Ahmad *et al.* [SNO Collaboration], *Phys. Rev. Lett.* **89**, 011301 (2002); K. Eguchi *et al.* [KamLAND Collaboration], *Phys. Rev. Lett.* **90**, 021802 (2003); M. H. Ahn *et al.* [K2K Collaboration], *Phys. Rev. Lett.* **90**, 041801 (2003).
- [2] For recent reviews on neutrino physics, see *e.g.*, V. Barger, D. Marfatia, and K. Whisnant, *Int. J. Mod. Phys. E* **12**, 569 (2003); R. N. Mohapatra and A. Y. Smirnov, *Annu. Rev. Nucl. Part. Sci.* **56**, 569 (2006); A. Strumia and F. Vissani, *hep-ph/0606054*; M. C. Gonzalez-Garcia and M. Maltoni, *Phys. Rep.* **460**, 1 (2008); Z. Z. Xing, *Int. J. Mod. Phys. A* **23**, 4255 (2008).
- [3] T. Abe *et al.* [American Linear Collider Group], *hep-ex/0106057*; J. A. Aguilar-Saavedra *et al.* [ECFA/DESY LC Physics Working Group], *hep-ph/0106315*; Koh Abe *et al.* [ACFA Linear Collider Working Group], *hep-ph/0109166*; ILC Technical Review Committee, second report, 2003, SLAC-R-606, February 2003.
- [4] G. Aarons *et al.* [ILC Collaboration], "International Linear Collider Reference Design Report Volume 2: Physics at the ILC," *arXiv: 0709.1893*; Brau *et al.* [ILC Collaboration], "ILC Reference Design Report Volume 1 - Executive Summary," *arXiv: 0712.1950*.
- [5] I. F. Ginzburg, *arXiv: 0912.4841*.
- [6] M. Cannoni, S. Kolb and O. Panella, *Phys. Rev. D* **68**, 096002 (2003); F. Deppisch *et al.*, *Phys. Rev. D* **69**, 054014 (2004); Y. B. Sun *et al.*, *JHEP* **0409**, 043 (2004); M. Cannoni, C. Carimalo, W. Da Silva and O. Panella, *Phys. Rev. D* **72**, 115004 (2005); *Erratum-ibid.*, *D* **72**, 119907 (2005); M. Cannoni and O. Panella, *Phys. Rev. D* **79**, 056001 (2009); J. Cao, L. Wu, J. Yang, *Nucl. Phys. B* **829**, 370 (2010).
- [7] Chong-Xing Yue, Yan-Ming Zhang and Hong Li, *J. Phys. G* **29**, 737 (2003); Guo-Li Liu, *arXiv: 1002.0659*.

- [8] P. M. Ferreira, R. B. Guedes, and R. Santos, *Phys. Rev. D* **75**, 055015 (2007); J. I. Aranda *et al.*, *Phys. Rev. D* **79**, 093009 (2009).
- [9] H. C. Cheng, I. Low, *JHEP* **0309**, 051 (2003); *JHEP* **0408**, 061 (2004); I. Low, *JHEP* **0410**, 067 (2004).
- [10] M. Schmaltz and D. Tucker-Smith, *Ann. Rev. Nucl. Part. Sci.* **55**, 229 (2005); M. Perelstein, *Prog. Part. Nucl. Phys.* **58**, 247 (2007).
- [11] J. Hubisz and P. Meade, *Phys. Rev. D* **71**, 035016 (2005); A. Belyaev, Chuan-Ren Chen, K. Tobe, C. P. Yuan, *Phys. Rev. D* **74**, 115020 (2006); J. Hubisz, P. Meade, A. Noble and M. Perelstein, *JHEP* **0601**, 135 (2006); J. Hubisz, S. J. Lee and G. Paz, *JHEP* **0606**, 041 (2006); M. Blanke, *et al.*, *JHEP* **0612**, 003 (2006).
- [12] M. Blanke *et al.*, *JHEP* **0701**, 066 (2007).
- [13] T. Goto, Y. Okada and Y. Yamamoto, *Phys. Lett. B* **670**, 378 (2009).
- [14] F. del Aguila, J. I. Illana and M. D. Jenkins, *JHEP* **0901**, 080 (2009); M. Blanke *et al.*, *Acta Phys. Polon. B* **41**, 657 (2010).
- [15] S. R. Choudhury, A. S. Cornell, A. Deandrea, N. Gaur and A. Goyal, *Phys. Rev. D* **75**, 055011 (2007); M. Blanke, A. J. Buras, B. Duling, A. Poschenrieder and C. Tarantino, *JHEP* **0705**, 013 (2007).
- [16] Chong-Xing Yue, Jin-Yan Liu, Shi-Hai Zhu, *Phys. Rev. D* **78**, 095006 (2008); Wei Liu, Chong-Xing Yue, Jiao Zhang, *Eur. Phys. J. C* **68**, 197 (2010).
- [17] T. Hahn, M. Perez-Victoria, *Computl. Phys. Commun.* **118**, 153 (1999); T. Hahn, *Nucl. Phys. Proc. Suppl.* **135**, 333 (2004).
- [18] W. M. Yao *et al.* [Particle Data Group], *J. Phys. G* **33**, 1(2006) and partial updat for the 2008 edition.

- [19] M. Blanke, A. J. Buras, *Acta Phys. Polon. B* **38**, 2923 (2007); Chong-Xing Yue, Nan Zhang, Shi-Hai Zhu, *Eur. Phys. J. C* **53**, 215 (2008).
- [20] O. Mena, S. J. Parke, *Phys. Rev. D* **69**, 117301(2004); J. D. Bjorken, P. F. Harrison, W. G. Scott, *Phys. Rev. D* **74**, 073012 (2006); R. N. Mohapatra *et al.*, *Rep. Prog. Phys.* **70**, 1757 (2007); C. Giunti, *Nucl. Phys. B, Proc. Suppl.* **169**, 309 (2007).
- [21] F. Ginzburg *et al.*, *Nucl. Instrum* **219**, 5 (1984); V. Telnov, *Nucl. Instrum. Methods Phys. Res. A* **294**, 72 (1990).
- [22] M. Blanke *et al.*, *Phys. Lett. B* **646**, 253 (2007); M. Blanke and A. J. Buras, *Acta Phys. Polon. B* **38**, 2923 (2007).
- [23] Wei Liu, Chong-Xing Yue, Hui-Di Yang, *Phys. Rev. D* **79**, 034008 (2009); Chong-Xing Yue, Jiao Zhang, Wei Liu, *Nucl. Phys. B* **832**, 342(2010)[ *arXiv: 1002.2010*].
- [24] X. L. Wang, Y. J. Zhang, H. L. Jin, Y. H. Xi, *Nucl. Phys. B* **807**, 210 (2009); **810**, 226 (2009); J. I. Aranda, A. Cordero-Cid, F. Ramirez-Zavaleta, J. J. Toscano, E. S. Tututi, *Phys. Rev. D* **81**, 077701 (2010).
- [25] G. Cacciapaglia, A. Deandrea, S.Rai Choudhury, N Gaur, *Phys. Rev. D* **81**, 075005 (2010).